

DIRECT MEASUREMENT OF FROZEN-IN FIELD IN THERMALLY POLED FIBRE DEVICES

Wei Xu, Danny Wong, Simon Fleming, Mark Janos⁺, and Kai-Ming Lo*

Australian Photonics Co-operative Research Centre
Optical Fibre Technology Centre
The University of Sydney
Australian Technology Park
Eveleigh, NSW 1430, Australia
Phone: +61 2 9351 1929
Fax: +61 2 9351 1910
Email: w.xu@ofc.usyd.edu.au

⁺Now with Uniphase Fibre Components

*Now with The University of Hong Kong

Abstract

We have experimentally verified existence of the frozen-in field in thermally poled fibre devices. The method can be used to measure both the magnitude and the direction of the frozen-in field as well as $\chi^{(3)}$. The relationship between $\chi^{(2)}$ and $\chi^{(3)}$ for thermally poled devices is also investigated in this paper.

1. Introduction

Large linear electro-optic (LEO) coefficients and second-order nonlinearities (SON) in silica fibres and waveguides will make possible many more active fibre and waveguide devices for WDM systems, for example, electro-optic modulators and switches, electrically tunable Bragg gratings and long periodic gratings, electrically tunable filters, frequency converters and parametric oscillators, etc. The creation of $\chi^{(2)}$ is explained by the establishment of a strong electric field in the anodic region of the thermally poled devices resulting from depletion of positive mobile charges under the applied poling field^[1]. Charge distributions in poled glasses were studied by the laser induced pressure pulse (LIPP)^[2] and the etching techniques^[3]. It is suggested that there are two layers of space charge: negatively charged depletion region and positively charged layer. However, these two methods give neither the direction nor the magnitude of the frozen-in field in poled glasses. Furthermore, it is still not clear whether $\chi^{(2)}$ is induced by high d.c. field via $\chi^{(3)}$ or orientation of dipoles, or a combination of both^[4]. This paper addresses these issues.

2. Experimental Setup and Theory

A free space Mach-Zehnder interferometer (MZI) operating at 632.8 nm wavelength was used for the measurement of the LEO coefficients in fibre devices, as shown in Fig. 1. Measurements of the magnitudes of modulated signals were taken on the quadrature points of the output of the Mach-Zehnder interferometer. A phase deviation $\Delta\phi$ about this quadrature point can be calculated from the peak-to-peak amplitude of the measured signal ΔV using

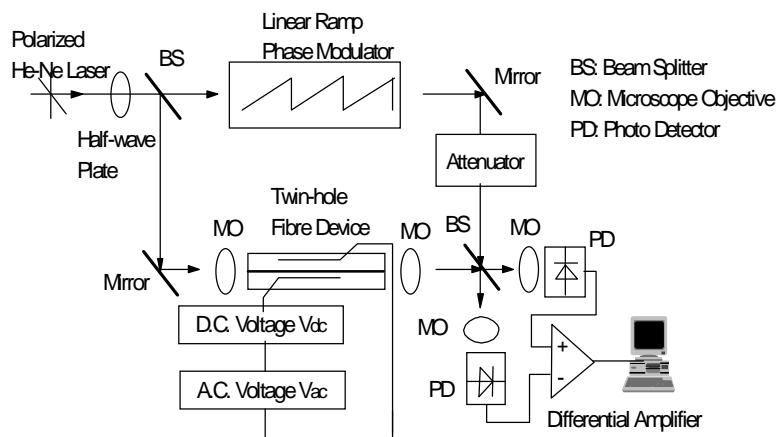


Fig. 1 Experimental Setup

A phase deviation $\Delta\phi$ about this quadrature point can be calculated from the peak-to-peak amplitude of the measured signal ΔV using

$$\Delta\phi = 2 \sin^{-1} \left(\frac{\Delta V}{V_{\max}} \right), \quad \text{----- (1)}$$

where V_{\max} is the peak-to-peak voltage at the output of the interferometer. From Equation 1, the electro-optic coefficient r is calculated using

$$r = \frac{\lambda d}{\pi V_{ac} L n^3} \Delta\phi, \quad \text{----- (2)}$$

where $\lambda = 632.8$ nm is the free-space optical wavelength of the light, V_{ac} is a peak-to-peak a.c. testing voltage, d is the distance between two electrodes, n is the refractive index of the core and L is the length of fibre devices. $\chi^{(2)}$ is related to r by the equation

$$\chi^{(2)} = \frac{n^4}{2} r. \quad \text{----- (3)}$$

The fibre devices were made from twin-hole fibres with two fine electrodes threaded into the two holes. In Fig.2, the electrode in the hole nearer to the core is denoted as the Active Electrode while the other is denoted as the Ground Electrode. Either a positive or a negative d.c. voltage, with respect to ground, can be applied to the Active Electrode for poling. The cross-sectional geometry of the devices and the distribution of the electrical fields in the devices before and after poling are shown in Fig. 2. The solid field lines correspond to a positive d.c. voltage being applied to the Active Electrode for poling. In Fig. 2b, the frozen-in field formed during poling is shown near to the Active Electrode. Obviously, a good overlap between the core and the frozen-in field results in a better electro-optic fibre device.

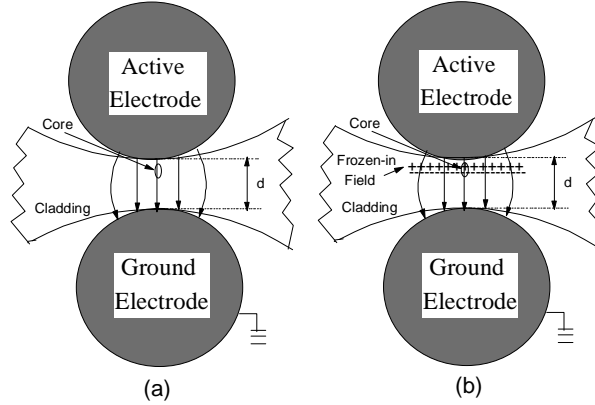


Fig. 2 Field distribution for a positive voltage applied to (a) an unpoled fibre device and (b) a poled fibre device with a frozen-in field.

In the experiments, an a.c. testing voltage V_{ac} of much smaller amplitude (~ 200 V) was superimposed onto the d.c. voltage V_{dc} . The linear EO modulation by the V_{ac} signal was then measured from the output of the MZI. Before poling, V_{dc} applied to the unpoled devices can cause a second-order nonlinearity;

$$\chi^{(2)} = \chi^{(3)} E_{dc}, \quad \text{----- (4)}$$

where $\chi^{(3)}$ is the third-order nonlinearity of the unpoled fibre devices, and $E_{dc} = V_{dc}/d$. Combining Eqs. (2), (3) and (4), $\chi^{(3)}$ for unpoled fibre devices can be expressed by means of

$$\chi^{(3)} = \frac{n\lambda d^2}{2LV_{\pi}V_{dc}}, \quad \text{----- (5)}$$

where V_π is the half-wave voltage corresponding to V_{dc} . As each quantity on the right side of Eq. (5) is measurable, the value of $\chi^{(3)}$ can be calculated. Fig.3a shows the measured $\chi^{(2)}$ of an unpoled device as a function of the applied V_{dc} . It follows from Eq.(4) that $\chi^{(3)}$ can be estimated from the slope of the plot. For our twin-hole fibre devices, the value of $\chi^{(3)}$ for the core is estimated to be $\sim 1.0 \% 10^{-22} (\text{m/V})^2$, which is in the same order of magnitude as $\chi^{(3)}$ for bulk silica glass of $1.8 \% 10^{-22} (\text{m/V})^2$. It is believed that the small discrepancy is caused by the existence of germanium in the fibre core and the error incurred in estimating the effective d due to the existence of air gaps between the electrodes and the cladding.

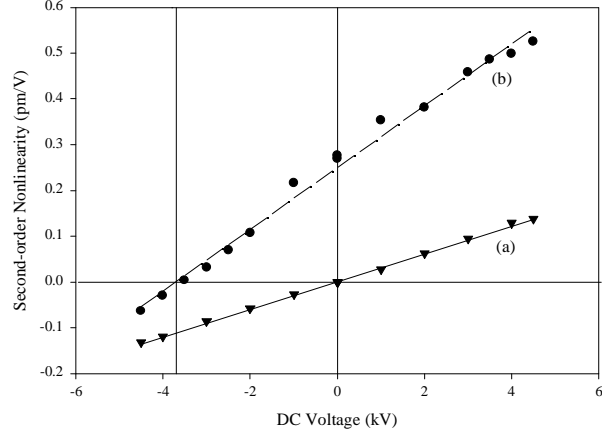


Fig. 3 (a) DC-caused $\chi^{(2)}$ before poling (solid line)
 (b) DC-caused $\chi^{(2)}$ after poling (dash line)

3. Results and Discussion

Fresh devices were poled at +3.5 kV d.c. voltage and at 250 °C for ~ 1 hour. After poling, a frozen-in field was induced in the devices. To investigate this frozen-in field in the poled fibre devices a small a.c. testing voltage V_{ac} was superimposed onto the d.c. voltage V_{dc} . Eqs (2) and (3) indicate that $\chi^{(2)}$ is proportional to $\Delta\phi$. It can be seen in Fig 3b that $\chi^{(2)}$ has a linear dependence on V_{dc} . $\chi^{(2)}$ became zero when the frozen-in field was balanced by a V_{dc} of -3.7 kV. So the magnitude of the frozen-in field in this device can be estimated as 200 V/ μm . The direction of the frozen-in field is the same as the direction of the external field caused by the positive V_{dc} . The formation of the frozen-in field may be explained as follows. When the fibre device was heated to a temperature of ≥ 200 °C, positive ions in the glass network became mobile and migrated to the cathode under the positive external poling field. The region near to the anode was depleted of positive ions and contained negatively charged centers (layers) embedded in the glass matrix. Due to the short distance between the anode and the negatively charged layers (\sim a few μm), there was a very strong electrical field between them. Ionization took place in the high field at the anodic region, and electrons migrated into the anode. The ionization process created a positively charged layer between the anode and the negatively charged depletion region. The frozen-in field then existed in the area between the positively and negatively charged regions, which was schematically shown in Fig 2b.

Interestingly in Fig. 3 the two slopes of the d.c.-caused EO modulation in the fibre devices before and after poling are different. This may be due to a change in the value of $\chi^{(3)}$ or due to the effect of the frozen-in field E_{frozen} , or a combination of both after poling through the modified relationship

$$\chi^{(2)} = \chi_{poled}^{(3)} E_{dc} + \chi_{induced}^{(2)} = \chi_{poled}^{(3)} (E_{dc} + E_{frozen}), \quad \text{----- (6)}$$

where $\chi_{\text{poled}}^{(3)}$ is the third-order nonlinearity of the poled devices, and $\chi_{\text{induced}}^{(2)}$ is the induced SON after poling.

Eq.(6) assumes the model of frozen-in electric field for poling. It follows that a change in material property might have occurred and hence the value of $\chi^{(3)}$. In the case of thermal poling, this could be associated with the migration of charges in the glass lattice as well as the re-distribution of residual frozen-in thermal stress. In either case, both the material property and the internal field can be changed. It would be interesting to investigate the relaxation time of these changes.

Using Eq. (6), with E_{frozen} being $200 \text{ V}/\mu\text{m}$ from Fig.3b, $\chi_{\text{poled}}^{(3)}$ is estimated to be $2.2 \% 10^{-22} (\text{m/V})^2$, which is 2.2 times of the value of $\chi^{(3)}$ for unpoled fibres. These estimations seem to fall in the expected range, which provides some support for the frozen-in field model of glass poling. From the microscopic point of view, random dipoles in the glass network are aligned under the frozen-in field. The aligned dipoles could give a higher macroscopic value of $\chi^{(3)}$ than randomly distributed dipoles. However, the evidence of possible changes in $\chi^{(3)}$ means that the contribution to $\chi^{(2)}$ is more than just due to the frozen-in field alone. We are currently including the changes of $\chi^{(3)}$ in the frozen-in field model for thermal poling of glass fibres.

4. Conclusions

To our best knowledge, it is believed that this paper is the first to report a method to measure both the magnitude and the direction of the frozen-in field in poled silica devices. The value of $\chi^{(3)}$ for unpoled silica devices can also be obtained from the same measurement. The method is suitable for any isotropic optical materials. The present result supports the frozen-in field model of glass thermal poling and indicates the possibility that $\chi^{(3)}$ of the glass fibre might have been varied by thermal poling.

5. Acknowledgements

The authors are grateful for the financial support from the Australian Photonics CRC, ABB and Transgrid Australia. The author Wei Xu would like to express thanks to the Department of Education, Employment and Training and Youth Affairs (DEETYA) of the Commonwealth Australia for the Overseas Postgraduate Research Scholarship (OPRS).

6. References

1. R. A. Myers, N. Mukherjee, and S. R. J. Brueck, "Large second-order nonlinearity in poled fused silica," *Opt. Lett.* **16**, 1732 (1991).
2. P. G. Kazansky, R. A. Smith, P. St. J. Russell, G. M. Yang, and G. M. Sessler, "Thermally poled silica glass: Laser-induced pressure pulse probe of charge-distribution," *Appl. Phys. Lett.* **68**, 269 (1996).
3. W. Margulis and F. Laurell, "Interferometric study of poled glass under etching," *Opt. Lett.* **21**, 1786 (1996).
4. P. G. Kazansky and V. Pruneri, "Fundamentals of glass poling: from self-organization to electric-field poling," *Bragg Gratings, Photosensitivity, and Poling in Glass Fibres and Waveguides: Applications and Fundamentals*, BtuC6, Page 305-307, Virginia, USA (1997).